Precision Polarimetry of Polarized ^{3}He

A thesis submitted in partial fulfillment of the requirement
for the degree of Bachelor of Arts / Science in Department from
The College of William and Mary

by

Nicholas Penthorn

Accepted for Honors
(Honors or no-Honors)

Todd Averett, Director

Henry Krakauer, Physics

Andreas Stathapoulos / Computer Science

Type in the name

Williamsburg, VA
April 22, 2014

Precision Polarimetry of Polarized ^{3}He

Nick Penthorn
Mentor Todd Averett

March 2014

Abstract

This work presents the progress of an experimental procedure designed to do precision polarimetry on polarized ^{3}He targets used in electron scattering experiments. Targets are polarized via spin-exchange optical pumping (SEOP), a process that uses circularly polarized laser light to give a spin polarization to the ^{3}He nuclei by way of spin transfer with a small amount of atomically polarized alkali metal in the cell. With this process, the polarization of a ^{3}He target that contains an alkali metal can be extracted via the frequency shift in the alkali metal's electron paramagnetic resonance (EPR) line; κ_0 is a constant that relates that frequency shift to the cell's polarization. Thus, the ultimate goal of this study is to reduce the uncertainty in $\kappa_{0,Rb}$ and $\kappa_{0,K}$ (the polarization constants associated with rubidium and potassium, respectively). Using a cylindrical cell and taking EPR measurements in two orthogonal cell orientations in an external magnetic holding field allows for the isolation of κ_0. The experimental setup entailed fabrication of an EPR frequency generator coil, a photodiode to detect light from EPR-driven electron transitions, and an oven to keep a portion of the alkali metal in a vaporous state at 210°C. Additionally, setup required optics to focus a polarizing laser tuned to the rubidium D_1 transition onto the cell for the purpose of SEOP. Relative cell polarizations are measured using NMR signals from the helium nuclei, a process that required making NMR generation and pickup coils. Finally, measurements were taken at EPR frequencies associated with ^{41}K, ^{39}K, and ^{85}Rb to determine the corresponding values of κ_0 and their uncertainties. The current research is focused on determining the temperature dependence of κ_0.

Contents

1 Introduction

The importance of precisely determing the nuclear polarization of a ^{3}He gas can't be understated. A free neutron has a lifetime of about 880 seconds, which makes careful study of neutrons challenging. Fortunately, the ^{3}He nucleus can be used as a reasonable model of the neutron. With two protons and one neutron, the ^{3}He nucleus in the ground state is a combination of three possible spin configurations: one with the proton spins aligned and the neutron spin anti-aligned, one with all particle spins aligned, and one with the proton spins anti-aligned. The most probable ^{3}He ground state ($\approx 90\%$) configuration is the latter, which has the net effect of the proton spins cancelling out and leaving the spin of the "free" neutron [7].
Physicists at Jefferson Lab in Newport News, Virginia take advantage of this phenomenon when conducting electron scattering experiments by using glass cells filled with polarized ^{3}He as the collision targets. Polarization here refers to the fraction of nuclei with the same spin state (with a spin axis defined by an external magnetic holding field), and the gas must be polarized in order to study spin-dependent neutron properties. Knowing the polarization of the helium gas is critical to JLab experiments, as it is currently the largest source of uncertainty.

1.1 Studies on κ_0

The polarization of a ^{3}He cell can be calculated by measuring the contribution of the polarized ^{3}He nuclei to the total magnetic field experienced by the alkali metal atoms. The greatest contribution to the uncertainty of this calculation is the dimensionless κ_0, which is a parameter used for a Fermi contact interaction between ^{3}He atoms and alkali metal atoms that is too complex to calculate from theory. It is unique to each alkali and has slight temperature dependence. Measurements have been made for κ_0 for ^{85}Rb with 1% uncertainty [1, 4], and for ^{39}K with 15% uncertainty [2, 3]. However, κ_0 for potassium was obtained indirectly by calculating a cell's polarization using $\kappa_{0,Rb}$ and solving backwards. The temperature dependence of $\kappa_{0,K}$ was assumed by the experimenters to be linear, although there is no data for higher temperatures conducive to spin exchange, around 235°C. No measurements have been made for κ_0 associated with ^{87}Rb, mainly because reading the small frequency shift due to its spin flip is quite difficult. The experimental design described in this paper makes it possible to precisely determine the values and temperature dependence of κ_0 for ^{41}K and ^{87}Rb, which drastically reduces the overall uncertainty in polarization measurements.

2 Experimental Setup

The existing stage for polarized ^{3}He cells was designed for two-chamber cells, described in Section 3.2. Two large helmholtz coils are mounted on either side of

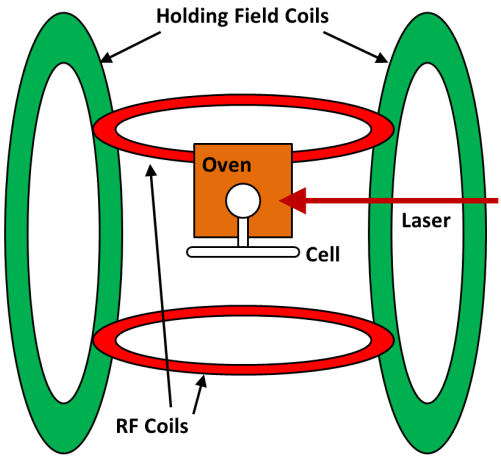

Figure 1: The original cell polarization setup, side view.

a rectangular oven to generate a magnetic holding field, and two smaller helmoltz coils are mounted above and below the oven to generate a radiofrequency NMR field. A polarizing laser beam is incident on one side of the oven, where there is a small window for the light to reach the cell within (Figure 1).

For a given ^{3}He cell, a number of tests must be performed to precisely determine its alkali ratio and locate resonances for EPR. Once the apparatus was constructed, it was necessary to run these tests and fine-tune the instrumentation to maximize signals. The procedure for testing the functionality of the setup was to measure EPR frequency shift as will eventually be done to lock down a κ_0 value, by separating EPR measurements with cell rotations (described above).
In order to do a full range of tests on a cylindrical cell using mostly magnetic signals, it was important in constructing the experimental apparatus to minimize the use of ferromagnetic materials. Measurement tools and instruments that were close to or inside of the cell oven also needed to be able to withstand the high temperatures of the cell. For gluing components together, a high-temperature liquid gasket used in car engines, RTV, was used. Wires and thermocouples were attached with high-temperature mylar tape and solid components were fabricated from Torlon plastic.

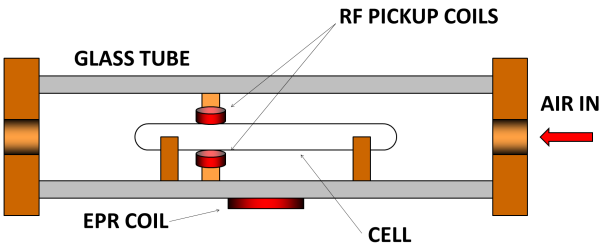

Figure 2: Cell oven: side view cross-section

2.1 Cell Oven

To keep some fraction of the alkali in a vaporous state and to increase the number of spin exchange interactions among nuclei, a ^{3}He cell needs to be maintained at an experimentally determined temperature between 185°C and 220°C. The cell oven (Figure 2) was made from a 1-foot-long Pyrex tube with a 2" square cross-section (inner dimension). The glass is 2.3 mm thick on the sides. Two square caps for sealing the ends of the oven were fabricated from 12.7 mm thick Torlon, each with a threaded hole for connection to a heated air line. The air temperature inside the oven was maintained by a PI feedback circuit controlled by a thermocouple secured to the middle of the cell in the oven with mylar. Cells are mounted inside the oven with two small rectangular Torlon stands, each with grooves cut into the top that matches the diameter of the cell it supports. The two stands are glued directly to the cell with RTV and the whole assembly is then glued to the floor of the oven. Because cells need to be studied in two different orientations, the end caps each have two plastic pegs protruding from their bottom edges, which fit into holes drilled into the fiberglass platform on which the oven rests. There are two sets of holes, one for each oven position.

Thermocouples attached to the cell in various locations showed a distinct temperature gradient between the end closest to the air supply and the opposite end. The close end was consistently measured as 220°C, while the far end was consistently measured as 190°C. This was accounted for by setting the temperature control box to 210 °C and having the feedback supplied by a thermocouple taped to the middle of the cell, close to the EPR coil. It was found that the average temperature of the cell could be found by averaging the temperatures of both ends, which matched the cell's midpoint temperature to within 0.5% uncertainty. This provided an average temperature of 210 °C across the cell, and specifically in the middle of the cell where the bulk of data was taken.

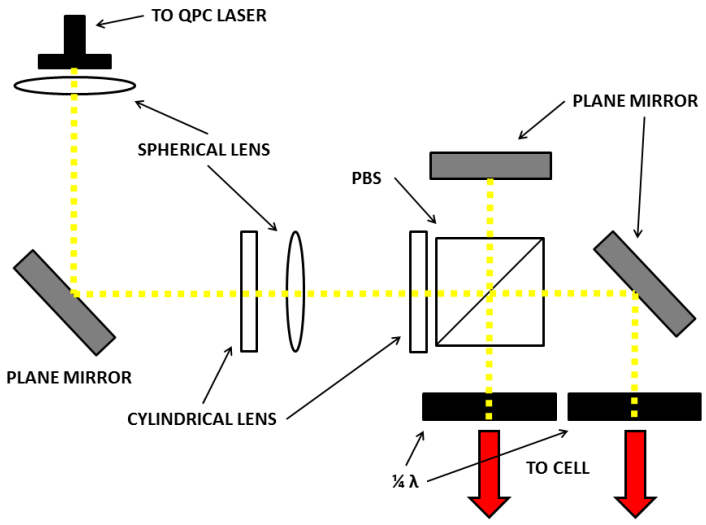

Figure 3: Primary beam diagram

2.2 Polarizing Optics

Cells were polarized with two laser beams, both tuned to the rubidium D_1 transition at 795 nm. The primary beam was aligned with the holding field and set to 25W output power. The probing beam, at 33W, was set at 45° to the holding field. Both beams were directed through polarizing beam splitters (PBS) to $\frac{1}{4}\lambda$ plates to make them circularly polarized. In the case of the primary laser, both beams emited from the PBS were directed to the cell (Figure 3). By contrast, the probing laser didn't need as much intensity and thus only one beam from the PBS was needed (Figure 4). Cylindrical lenses were added to focus the circular profile of the beams down to elliptical profiles with the purpose of maximizing the light incident on the cell. The probing beam and its optics were mounted on a non-ferromagnetic optical breadboard which was in turn mounted on a wooden platform. The distance from the probing laser to the center of the cell was 26". The optics associated with the primary beam were mounted on an optical table sufficiently far away from the cell (163 cm) that it wouldn't interfere with the generated magnetic fields.

2.3 NMR

To generate the radiofrequency magnetic signal used for spin flips and AM/FM sweeps, the existing NMR generation coils weren't used because of their position in relation to the EPR coil. Two Helmholtz coils were constructed at right angles

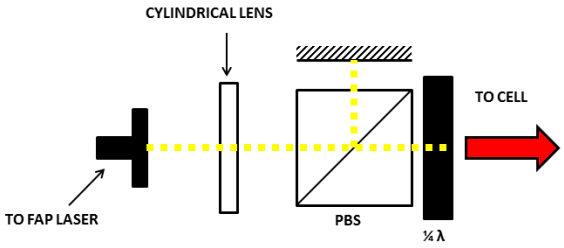

Figure 4: Probing beam diagram

to the holding field. Each coil was 51 cm high and 56 cm wide with 8 turns of copper wire. They were mounted onto the oven platform with plastic brackets at each of their four corners. When wired together, they were measured to have an inductance of 231.4 μH and a resistance of 593 mΩ. The corresponding RF pickup coils were each 100 turns of 34-gauge copper wire wound around a 1/2" diameter torlon disk and secured in place with a layer of RTV. Together, the coils had an inductance of 369 μH and a resistance of 724 mΩ. Because the NMR signal quickly drops away the further it is measured from the cell, the pickup coils were mounted inside the oven, orthogonal to both the holding field and the RF field, using a thin torlon frame. The RF pickup coils had a small amount of vertical adjustability (around 6 mm) to ensure that the coils were as close as possible to the cell.

2.4 EPR

The EPR frequency signal was generated with a single coil of 22 gauge copper wire wound with 10 turns around a 4.5 cm diameter torlon disk. The coil was mounted to the underside of the oven at the exact center with mylar tape. Its inductance and resistance were measured to be 9.2 μH and 184 mΩ, respectively. A photodiode was mounted above the cell and in line with the EPR coil on a fiberglass platform. Light from the cell reached the photodiode through a 5 cm diameter hole in the platform and a focusing lens. The lens was 16 cm away from the top surface of the oven and the photodiode was 20 cm away. The photodiode was equipped with D_2 filters to detect fluorescence from EPR-driven alkali electron transitions.

3 Methods

Target cells are polarized via spin-exchange optical pumping (SEOP), a multi-step process in which circularly polarized laser light transfers spin to the helium nuclei. In the first step of this process, an alkali metal is added to the cell which has a high spin exchange rate. The alkali metal, usually rubidium, is

optically pumped and transfers spin to the helium through a contact interaction [8]. The lasers used for optical pumping are therefore tuned to the rubidium D_1 transition, 795 nm. The polarization can be further improved by adding potassium, which has a slower spin relaxation rate than that of rubidium [3]. With a mix of the two alkali metals, rubidium atoms will be directly polarized by the D_1 light and exchange their spins with potassium atoms, which then exchange spins with helium atoms. With continuous optical pumping under optimal conditions, the majority of helium atoms in a cell will have the same spin.

3.1 EPR

The addition of alkali metals to a ^{3}He cell has the added benefit of measuring the cell's polarization indirectly with electron paramagnetic resonance (EPR). In the presence of a magnetic holding field, the alkali metal atom's hyperfine energy levels experience Zeeman splitting, with the energy difference between levels proportional to the strength of the magnetic field. Each polarized ^{3}He nucleus contributes to the local field strength, and so the alkali metal atoms' hyperfine levels will be spread apart due to both the external holding field and each of the ^{3}He nuclei. Thus, the energy spacing between alkali hyperfine levels is proportional to the ^{3}He polarization. The alkali hyperfine levels can be determined by driving a particular hyperfine transition, using a magnetic field oscillating at an EPR frequency, and picking up the frequency of emitted light at resonance with a photodiode. The EPR signal drives electrons up to a state that allows them to absorb the polarizing laser's D_1 light, and alkali atoms can be further excited through collisional mixing and eventually emit D_1 and D_2 light. A peak in D_2 intensity at 780 nm indicates resonance, and consequently the photodiode has filters to block out D_1 light from the laser.

3.2 EPR-AFP

To isolate the total ^{3}He contribution to the field, the ^{3}He spins can be flipped 180° with respect to the holding field and the new hyperfine levels can be measured. When the spins are flipped using the adiabatic fast passage (AFP) technique (described in section II.A), their spins transition from being parallel to the holding field to being antiparallel. It follows that the shift in alkali hyperfine levels will reflect the ^{3}He field contribution [1].
Because the hyperfine levels shift due to the spin flip, so too does the EPR frequency required to drive electron hyperfine transitions. It is therefore necessary to use a lock-in amplifier to adjust the EPR frequency as needed, with feedback provided by the photodiode. The quantity measured in AFP-EPR is actually the EPR frequency used by the system and it is the shift in EPR frequency that is used to calculate the cell's polarization. A typical target cell consists of a spherical "pumping chamber" connected by a thin glass tube to a cylindrical "target chamber". The pumping chamber is optically pumped during experiments and the electron beam is directed through the target chamber. For a cell

of this variety, the cell geometry is can be approximated as a perfect sphere and the EPR frequency shift is related to the polarization by [1]

$$\Delta\nu_{EPR} = \frac{8\pi}{3}\kappa_0\mu_{He}\mu_0 n_p P_{He}\frac{d\nu}{dB}. \tag{1}$$

In (1), μ_{He} is the magnetic moment of helium, μ_0 is the vacuum permeability, n_p is the density of ^{3}He in the pumping chamber, P_{He} is the helium's polarization, and $\frac{d\nu}{dB}$ is the derivative of EPR frequency with respect to the holding field. From this expression, one can understand κ_0 as a frequency shift enhancement factor, the enhancement due to collisions between helium and alkali atoms.

3.3 Isolating κ_0

For a non-spherical cell, the EPR frequency shift depends on the cell geometry and how it is aligned with the holding field. The polarization, however, remains the same regardless of the cell's orientation within the holding field. An infinitely long cylindrical cell is the idealized version of the cells used in this study. When the cell axis is aligned with the holding field, the frequency shift is given by

$$\Delta\nu_{EPR_{\parallel}} = \mu_{He}n_{He}\mu_0 P_{He}\frac{d\nu}{dB}(\frac{8\pi}{3}\kappa_0 + (4\pi - \frac{8\pi}{3})), \tag{2}$$

whereas if the cell axis is perpendicular to the field then the expression becomes

$$\Delta\nu_{EPR_{\perp}} = \mu_{He}n_{He}\mu_0 P_{He}\frac{d\nu}{dB}(\frac{8\pi}{3}\kappa_0 + (2\pi - \frac{8\pi}{3})). \tag{3}$$

Armed with this information, it is possible to isolate the value of κ_0 by taking EPR measurements in both orientations and dividing one expression by the other. The cell polarization, which isn't known with high precision, cancels out in both the numerator and denominator and what's left are known constants and geometrical terms. In practice, it has been shown that a cylindrical cell with a length of 18 cm and a diameter of 1.2 cm has a magnetization that differs from that of an infinitely long cylinder by less than 0.6% [1]. The fact that optical pumping is done with a laser aligned with the holding field direction implies that it is not practical to do continuous optical pumping on a cell when it is in its perpendicular orientation; a small fraction of the cell's surface would receive direct laser light, and thus the cell would sustain losses in polarization between measurements. The solution is to use two polarized lasers, a primary laser to polarize the cell before measurements and a probing laser to optically pump the cell during measurements. The primary beam is in the direction of the holding field, and the probing beam is set at 45° to the holding field (Figure 5). The probing laser's position allows it to optically pump the cell in both orientations with identical efficiency. Figure 6 shows the orientations of the cell and laser directions with respect to the holding field and NMR RF field, each generated by a set of Helmholtz coils.

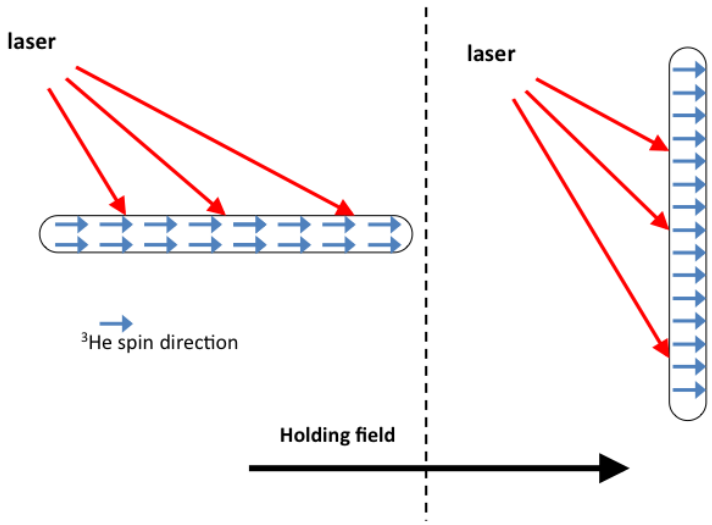

Figure 5: Detail of cell positions and the directions of the magnetic field due to ^{3}He polarization.

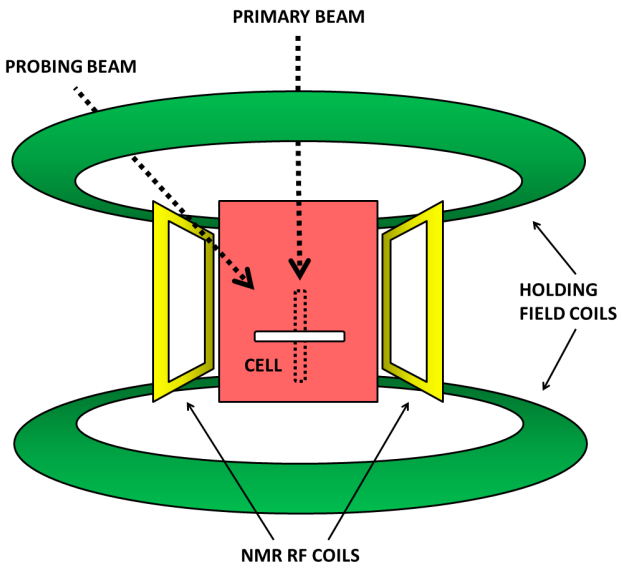

Figure 6: Cell orientations within RF and holding fields (viewed from above).

In practice, it was found that the probing laser was capable of polarizing cells with an efficiency at least equal to that of the pumping laser, given the space constraints of the lab setup. Thus, the probing laser was used to initially polarize the cell and also to maintain polarization during measurements. The pumping laser was omitted as a redundancy.

3.4 Flipping ^{3}He Spins

To reverse the direction of ^{3}He polarization, a radiofrequency field is applied to the cell and the value of the holding field is swept through ^{3}He nuclear resonance. In the absence of any RF field, the nuclear spin axes will precess about the holding field at the Larmor frequency [5, 6]

$$\omega_0 = \gamma H_0. \tag{4}$$

In (4), γ is helium's gyromagnetic ratio and H_0 is the holding field magnitude. In a reference frame rotating about an axis aligned with the holding field direction at ω_{RF} ,the effective magnetic field magnitude experienced by nuclei in the cell is

$$H_{eff} = H_0 - \frac{\omega_{RF}}{\gamma}. \tag{5}$$

When the RF field is turned on, the magnitude of the new field is

$$H_{tot} = \sqrt{H_{eff}^2 + H_1^2}. \tag{6}$$

In (6), H_1 is the magnitude of the RF field.
The initial value of H_0 is set so that $H_0 < \frac{\omega_{RF}}{\gamma}$ and it is gradually increased; when $H_0 = \frac{\omega_{RF}}{\gamma}$, $H_{eff} = 0$. At this point the nuclei are only acted on by H_1 and the spins align themselves with the oscillating RF field. When H_0 is increased further, H_{eff} becomes negative and the spins pick up a component that is antiparallel to the holding field. In this way the spin direction is flipped 180°. The adiabatic fast passage (AFP) conditions for a spin flip require that the holding field magnitude changes quickly enough so the spin doesn't have time to relax to its previous alignment, yet much slower than the Larmor frequency so the spin can follow H_{eff} as it rotates [5, 6].
A side effect of the AFP technique is the slight loss in polarization that occurs each time it is applied to a ^{3}He cell. This polarization loss is dependent on the "lifetime" of the cell (as determined by the time it takes for the cell polarization to drop to $\frac{1}{e}$ of its original value once the pumping laser is turned off) and the number of spin reversals performed.

3.5 NMR-AFP

A method of measuring polarization loss, NMR measurements also implement spin flips in the AFP regime by ramping the holding field. As the helium nuclear spin axes rotate, they collectively induce a voltage in pickup coils mounted orthoganally to the holding field coils and RF coils. The maximum (absolute value) induced voltage occurs at the point when the spins are halfway through their rotation, at 90° to the holding field. Because the holding field ramps up and then back down to its original value, a typical NMR signal has two peaks that indicate where the spins have rotated through 90° (Figure 7). The peak heights are proportional to the ^{3}He polarization, so the change in NMR peak heights over time is a good measure of how much polarization is lost during measurements.

3.6 Determining the Alkali Ratio

When a cell is filled with ^{3}He and alkali metals, the ratio of quantities of rubidium and potassium isn't immediately known. Fortunately there is a procedure to retroactively determine the alkali ratio using EPR. During an amplitude modulated (AM) sweep, the holding field is slowly increased from its starting value and the photodiode records the amount of light given off by alkali electron transitions with a constant EPR frequency. At certain field values, resonances occur and the light intensity drops. The light intensity as a function of holding field strength becomes a series of negative peaks on an otherwise constant level of background noise (Figure 8). Each peak represents one Zeeman transition

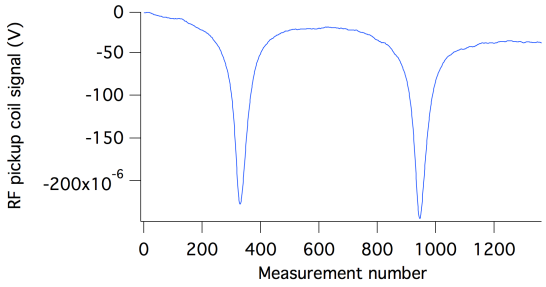

Figure 7: NMR signal as the holding field is swept up and back down with constant NMR frequency.

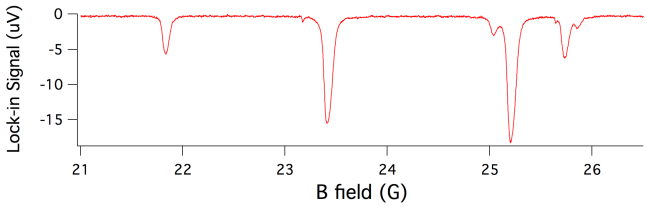

Figure 8: AM sweep on cell "Symon". Peaks from left to right are: ^{41}K ($m_F = -1 \leftrightarrow -2$), ^{39}K ($m_F = -1 \leftrightarrow -2$), ^{39}K ($m_F = 0 \leftrightarrow -1$), ^{87}Rb ($m_F = -1 \leftrightarrow -2$), ^{87}Rb ($m_F = 1 \leftrightarrow 0$), and ^{87}Rb ($m_F = 2 \leftrightarrow 1$).

of a particular alkali metal, and the peaks can be used to determine the alkali ratio [3]:

$$\mathcal{D} = \frac{\sum(^{39}\mathrm{K}) + \sum(^{41}\mathrm{K})}{\sum(^{87}\mathrm{Rb}) + \sum(^{85}\mathrm{Rb})}. \tag{7}$$

In (7), $\sum(^{39}\mathrm{K}) + \sum^{41}\mathrm{K})$ is the sum of potassium peak areas and $\sum(^{87}\mathrm{Rb}) + \sum(^{85}\mathrm{Rb})$ is the sum of rubidium peak areas.
In practice, the peaks of ^{85}Rb are at a much higher holding field value than what is generated (around 35 G). It is therefore a good approximation to substitute the denominator of (7) with $\frac{\sum(^{87}\mathrm{Rb})}{0.2783}$, where 0.2783 is the natural isotopic fraction of ^{87}Rb. The areas under the peaks are found by fitting each peak with a Lorentzian profile [10]. The areas are calculated while decrementing the voltage supply to the EPR RF frequency signal. The peak areas used in (7) are the extrapolated areas that would occur at $\mathrm{V}_{EPR} = 0$.

3.7 Finding Resonances for EPR

Before the lock-in amplifier can lock on a particular resonant frequency for EPR, all or most of the frequencies for rubidium and potassium must be located. The process is similar to the one used to determine the alkali ratio. Instead of sweeping the holding field, the RF frequency is increased with the holding field

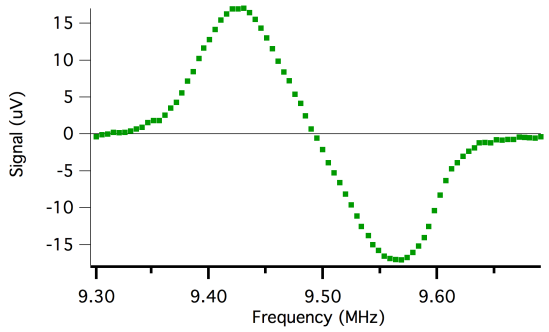

Figure 9: An FM sweep used to locate the ^{39}K ($m_F = -1 \leftrightarrow -2$) resonance, shown here to be at around 9.48 MHz.

maintained at 13 G. The plot of photodiode signal as a function of RF frequency is the derivative of the plot made by an AM sweep. The points where the signal crosses the zero signal mark (AM sweep minima) represent points of resonance (Figure 9). Although both frequency modulated (FM) sweeps and AM sweeps show where resonances are, the FM sweep is more useful in this regard because the lock-in amplifier locks onto a frequency, not a holding field value.

3.8 Tests on Cell "Symon"

To test and calibrate the system, a cylindrical cell 20 cm in length and 1.3 cm in outer diameter was filled with ^{3}He gas and small quantity of a rubidium-potassium mixture. The cell inner volume was 12.88 mL and the ^{3}He density was found to be 7.97 amg. The cell's alkali ratio was determined with an AM sweep from 20 G to 27 G at an RF frequency of 17.5 MHz in V_{rf} increments of 2V from 12V to 2V.

The first test was to optically pump the cell at 185 °C with the primary laser overnight, then do several AFP-NMR sweeps to determine if there was a high enough cell polarization to perform the necessary measurements. The NMR RF frequency was set to 53.6 kHz at $0.5V_{rms}$ and the holding field was ramped from 13 G to 21 G at a rate of 3 G/s. Studying the NMR signal also gave an indication as to the cell's polarization loss during spin flips.

Next, the EPR coil was tested by locating resonances with an FM sweep from 8.9 MHz to 9.7 MHz and locking onto them one at a time. The last functionality test was to perform a spin flip and adjust the lock-in to maximize the photodiode signal. As a final test of the whole system, the lock-in was locked onto the ^{39}K ($m_F = -1 \leftrightarrow -2$) transition and the primary beam was turned off. An AFP-NMR measurement was taken, followed by an AFP-EPR spin flip, followed by another AFP-NMR measurement in succession with the probing beam on. Then the cell was rotated 90° to its second position and measurements were repeated for a total of 7 measurements of alternating cell positions. Polarization losses and EPR signals were recorded.

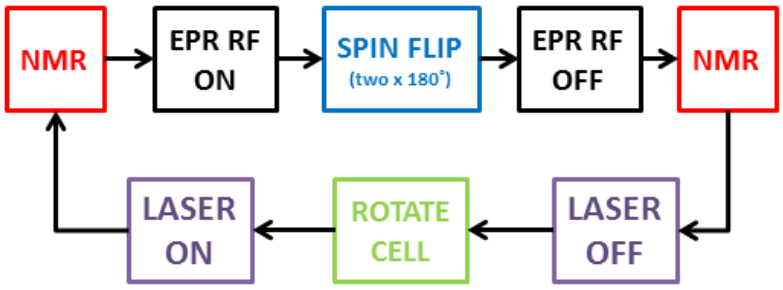

Figure 10: The procedure for recording EPR data using spin flips.

4 Measurements for κ_0

To begin taking the official NMR and EPR data for determining κ_0, the cell temperature was raised to 210°C and the probing beam was left on to optically pump the cell overnight. The spin flip procedure, shown in Figure 10, was carried out for each alkali species of interest.

4.1 The Spin Flip Procedure

Initially, an FM sweep across the general area of the EPR frequency of the alkali species of interest was performed to determine the EPR lock-in frequency and optimize the phase between the signal and noise channels of the lock-in. An AFP-NMR measurement was taken to serve as the baseline polarization, which is compared to all subsequent AFP-NMR data during spin flips as a relative polarization measurement. Next, the EPR RF field was turned on. After approximately five seconds, a spin flip was induced in the cell. The EPR RF field was turned off following another pause of approximately five seconds, and AFP-NMR data was taken. The probing beam was turned off, the cell was rotated, the probing beam was turned back on, AFP-NMR data was taken, the EPR RF field was turned on, and the process was repeated.

4.2 Correcting for Polarization Loss

During the spin flip procedure, several mechanisms were working to lower the cell's polarization. In EPR data, this polarization loss manifested itself in a net decrease in frequency shift. Whenever the probing beam was off for a cell rotation, the natural spin relaxation of the alkali atoms caused a drop in polarization. Similarly, there was polarization loss whenever the alkali spins were anti-aligned with the holding field. Since both AFP-EPR and AFP-NMR measurements rely on spin flips, both techniques contributed to a total polarization loss. A simple measurement of the EPR frequency over time with the helium

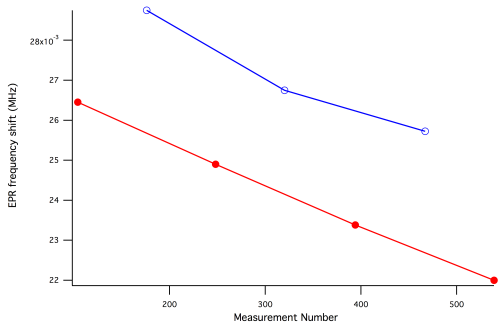

Figure 11: The EPR frequency shift is shown to decrease with time due to polarization loss. Blue line: $\Delta\nu_{EPR_{\parallel}}$. Red line: $\Delta\nu_{EPR_{\perp}}$. One measurement on the x-axis is 0.6 seconds.

spins anti-aligned showed a loss rate of 0.013% per second, which corresponds to 0.26% loss per spin flip. A third mechanism is the EPR RF field, which slowly depolarizes the cell whenever it is on. EPR data taken while the EPR RF field was on showed a negligible loss due to this effect. A final factor, which was unforeseen during measurements, seems to have the biggest contribution to the cell's polarization loss: the cell rotation. If the cell is rotated too quickly, then the AFP conditions for the helium nuclei to stay aligned with the holding field aren't met.

The relative polarization measurements provided by the frequent NMR data was thought to be an excellent way to correct for any loss in polarization. The NMR peak heights were to be graphed as a function of time and fitted linearly, with the goal of using the slope of the fit line to modify the frequency shift values so that they were approximately constant with time. However, the RF pickup coils mounted inside the cell oven were not fixed at the exact center of the cell, nor were they exactly orthogonal to the NMR coils; therefore, NMR data showed discontinuities in polarization each time the cell was rotated. The NMR data was useful in showing the polarization loss of the cell in one set orientation, but not in showing the polarization loss as the cell was rotated. Fortunately, the values of $\Delta\nu_{EPR}$ themselves could be used to determine the polarization loss as they were shown to decrease linearly with time (Figure 11, shown here using ^{39}K). Although this way of correcting the frequency shifts introduced more uncertainty into the study, the uncertainties were small enough that it would suffice.

5 Results

The AM sweep showed remarkably well-defined alkali peaks, most notably the ^{87}Rb $(-1 \leftrightarrow -2)$ transition, which was previously unresolvable. The relatively

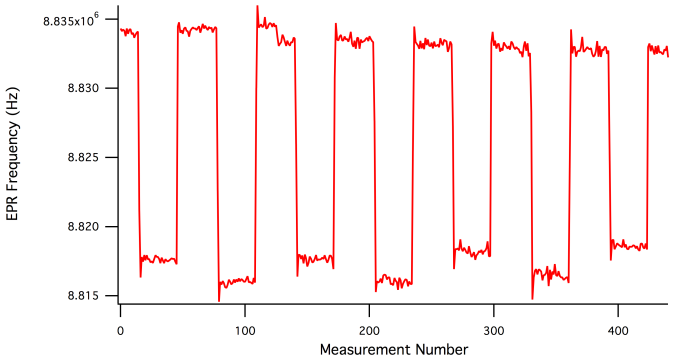

Figure 12: EPR-AFP data. The large discontinuities represent spin flips, and one measurement on the x-axis takes 0.6 seconds.

high amount of rubidium reflects the higher vaporization temperature of potassium: at the average cell temperature, there was more rubidium vapor present in the cell. The cell alkali ratio (potassium to rubidium) was found to be $\mathcal{D} = 0.723$ at 185°C.

NMR-AFP tests showed that the usable signal detected by the RF pickup coils was small when compared to the background noise. The huge amount of noise was a result of imperfect alignment of the pickup coils within the larger RF and holding fields. The signal-to-noise ratio was made worse by the low initial cell temperature of 185°C. At that temperature, a small amount of rubidium and almost no potassium were in vapor form, which led to a low spin exchange rate. Therefore, the small signal size reflected a very low cell polarization rather than defects in the instrumentation. Increasing the signal gain and adjusting the lock-in phase to put as much of the noise into the lock-in's y channel produced a clean NMR signal with the characteristic twin peaks (Figure 7). During the measurements for κ_0, the cell temperature was at 210°C and the NMR signals were accordingly better defined. The steady decline of induced voltage in the RF pickup coils from the first measurement to the last was due to polarization loss.

An FM sweep from 8.5 MHz to 10 MHz at 14 V with a 13 G holding field showed several resonances, some of which were too close together to properly resolve. The three largest slopes, consistent with the AM sweep, were ^{41}K $(1 \leftrightarrow 0)$, ^{39}K $(-1 \leftrightarrow -2)$, and ^{87}Rb $(-1 \leftrightarrow -2)$ at 8.8 MHz, 9.5 MHz, and 9.1 MHz, respectively.

The ^{39}K $(-1 \leftrightarrow -2)$, ^{87}Rb $(-1 \leftrightarrow -2)$, and ^{41}K $(1 \leftrightarrow 0)$ transitions were successfully locked on, and the EPR frequency shifts $\Delta\nu_{EPR_\perp}$ and $\Delta\nu_{EPR_\parallel}$ were measured over 7 spin flips for each alkali species. The results for ^{41}K are pictured in Figure 12 and summarized in Table 1.

Similar data was taken for ^{39}K $(-1 \leftrightarrow -2)$ at 210°C. The NMR data taken in between EPR measurements was inconclusive due to the errors created when

Table 1: EPR Frequency Shifts

Measurement	Cell Orientation	$\Delta\nu_{EPR}$ (kHz)
1	$\perp$	16.56 ± 0.044
2	$\parallel$	18.480 ± 0.044
3	$\perp$	15.80 ± 0.056
4	$\parallel$	17.20 ± 0.062
5	$\perp$	14.90 ± 0.066
6	$\parallel$	16.36 ± 0.081
7	$\perp$	14.10 ± 0.065

Table 2: κ_0

Alkali Species	κ_0(210 °C)
^{87}Rb	7.3 ± 0.33
^{39}K	8.8 ± 0.15
^{41}K	6.9 ± 0.19

rotating the cell.

The value of $\Delta\nu_{EPR}$ for each spin flip was computed using a weighted average of the two shifts on either side of the flip. These averaged values were plotted as a function of EPR measurement number (one measurement = 0.6 seconds) and fitted linearly. The slope of the fit line was used to correct for polarization loss, and then the corrected values were combined with a weighted average to obtain the final values of $\Delta\nu_{EPR_\perp}$ and $\Delta\nu_{EPR_\parallel}$. The value of κ_0 was obtained directly from these two values. As corroboration for the apparently low polarization losses seen in the EPR measurements, the AFP polarization loss was also calculated by running ten NMR sweeps in rapid succession (0.01 minutes between sweeps). The average polarization loss per measurement was found to be 0.74% for the up sweep and 0.76% for the down sweep.

Finally, the EPR data and $\Delta\nu_{EPR}$ values were sufficiently precise to calculate the values of κ_0 at 210 °C (Table 2):

6 Ongoing Tests with Cell "Wurst"

In order to reach a higher level of precision than was possible with the experimental setup used in the above sections, a new experimental apparatus was constructed. Most notably, new NMR pickup coils were made to address the errors in NMR measurements mentioned in Section 5. Both of these coils were constructed from 160 turns of 22-gauge copper wire, wrapped on fiberglass frames with cross-sectional area of 23 cm by 4 cm. Instead of being mounted inside the cell oven, these coils were externally mounted on a frame of threaded fiberglass rods. The new design allowed for a higher sensitivity to NMR signals, as well as improved adjustability to eliminate noise from the RF coils or holding

Table 3: $\kappa_{0,^{39}K}$

Cell Temp. ($^{\circ}C$)	κ_0	Published [2]	Theory [9]
210	8.8 ± 0.15	6.1 ± 0.91	> 8.5
220	9.5 ± 0.28	6.2 ± 0.93	> 8.5

field. In addition, the photodiode and EPR coil were fixed to the same fiberglass frame, ensuring no relative motion that could confound measurements. Cell "Wurst" was a hybrid cell with a length of 21 cm and a 2.45 cm diameter, with an internal volume of 210 mL. The advantage of using a larger cell is that all signals from the cell, both NMR and EPR, will be much larger in relation to background noise. Using the larger cell with the new apparatus will guarantee values of κ_0 with higher precision. To check consistency, κ_0 was calculated at 220 °C and found to be 9.4 ± 0.

7 Conclusions

The AM sweep on the test cell showed that the resonance spectrum was very well-defined; with the standard setup (spherical cell, temperature at 235 °C, V_{EPR} = 14V) the sweep was incapable of distinguishing between rubidium transitions. With the new setup, three rubidium transitions were resolved. It is evident from the EPR measurements that there is little or no system bias between the two cell orientations. The change in both $\Delta\nu_{EPR_\perp}$ and $\Delta\nu_{EPR_\parallel}$ between measurements in the same orientation was small, and the change in both exhibited a constant downward trend, consistent with natural polarization loss (Figure 11).
From the AFP loss study with NMR, the consistently low polarization loss was a good sign for the functionality of the system. These low polarization losses are key for measurements of κ_0, where depolarization makes the EPR and NMR signals more difficult to resolve.

The calculated values of κ_0 are promising. The goal of less than 5% uncertainty has been met for all studied alkali isotopes. These results are an encouraging first step, as they demonstrate the possibility of determining κ_0 for any isotope of rubidium or potassium. It is important to note a rather perplexing deviation from the established value of $\kappa_{0,^{39}K}$: at 210 °C, the calculated value is 3σ away from the expected value of 6.1 ± 0.91, extrapolated from published data (Table 3) [2].

A possible explanation is that the alkali hyperfine transition I used in my measurements was simply misidentified, and that it was in reality a different transition with a very similar EPR frequency. The possibility of a miscalibration of the system was ruled out after comparing the measured ν_{EPR} values with published data [10]. A more extreme explanation is that κ_0 does not in fact increase linearly with temperature. Because previous studies had mea-

sured κ_0 at temperatures between 70 and 170 °C, it was only assumed that the linear relationship would continue for higher temperatures. It should be noted that my value corroborates well with the existing theory-based estimate of $\kappa_{0,^{39}K}(100°\text{C}) = 8.5$ [9], which may indicate that my calculation isn't far off. Once the question of the $\kappa_{0,^{39}K}$ is resolved, the next step in the process is to take measurements at lower temperatures to determine the temperature dependence of κ_0. Measurements of κ_0 for ^{41}K, ^{39}K, and ^{87}Rb with improved precision are underway.

References

[1] M. V. Romalis and G. D. Cates, Phys. Rev. A **58** (1998) 3004.

[2] E. Babcock *et al*, Phys. Rev. A **71** (2005) 013414.

[3] A. B. Baranga *et al*, Phys. Rev. Lett. **80** (1998) 2801.

[4] A. S. Barton *et al*, Phys. Rev. A **49** (1994) 2766.

[5] A. Abragam, *Principles of Nuclear Magnetism* (Oxford University Press, 1990).

[6] M. J. Duer, *Solid-State NMR Spectroscopy* (Blackwell Publishing, 2004).

[7] J. Friar, B. Gibson *et al*, Phys. Rev C **42** (1990) 2310.

[8] T. Walker and W. Happer, Rev. Mod. Phys. **69** (1997) 629.

[9] T. Walker, Phys. Rev. A **40** (1989) 4959.

[10] J. Singh, Ph.D. thesis, University of Virginia (2010).